AIMS Mathematics, 8(2): 4575–4595.
DOI: 10.3934/math.2023226
Received: 23 October 2022
Revised: 22 November 2022
Accepted: 26 November 2022
Published: 06 December 2022

http://www.aimspress.com/journal/Math

Research article

A numerical study of swirling axisymmetric flow characteristics in a cylinder with suspended PEG based magnetite and oxides nanoparticles

C. S. K. Raju[1a,1b,†], S.V. Siva Rama Raju[2], S. Mamatha Upadhya[3], N. Ameer Ahammad[4], Nehad Ali Shah[5,†] and Thongchai Botmart[6,*]

[1a] School of Mechanical Engineering, Hanyang University, 222 Wangsimni-ro, Seongdong-gu, Seoul 04763, Republic of Korea
[1b] Department of Mathematics, GITAM School of Science, GITAM University, Bangalore-Karnataka, India-561205
[2] Academic Support Department, Abu Dhabi Polytechnic, Abu Dhabi, UAE
[3] Faculty of Mathematics, School of Management Studies, Kristu Jayanti College (Autonomous),15 Autonomous PO, K. Narayanapura, Kothanur, Bengaluru, 16 Karnataka 560077, India
[4] Department of Mathematics, Faculty of Science, University of Tabuk, P.O. Box741, Tabuk 71491, Saudi Arabia
[5] Department of Mechanical Engineering, Sejong University, Seoul 05006, South Korea
[6] Department of Mathematics, Faculty of Science, Khon Kaen University, Khon Kaen 40002, Thailand

*** Correspondence:** Email: thongbo@kku.ac.th.

† These two authors contributed equally and are co-first authors.

Abstract: For entire heat transfer practitioners from the last ten years, heat transmission performance in cooling and heating applications has become foremost concern. Hence, research towards innovative heat transference fluids is enormously powerful and stimulating. This study examines flow and thermal management in axisymmetric magneto hydrodynamic Polyethylene glycol (PEG) based hybrid nanofluid flow induced by a swirling cylinder. Flow and heat transfer is analyzed and compared for PEG+ $Cu_2O + MgO$ and PEG+Graphene+ $Cu + Ag$ hybrid nanofluid flow. Shooting

technique (R-K 4th order) is applied to work out the flow equations numerically. Simulated results are demonstrated via graphs. The computational results are validated with the published research work and found a modest concurrence. The foremost outcome of this investigation is found to be the axial, swirl and radial velocities in hybrid nanofluid are observed to decay with improvement in Reynolds number, nanofluid volume fraction and magnetic parameter. Platelet shaped nanoparticle colloidal suspension exhibit more decaying axial, swirl and radial velocity compared to spherical shaped nanoparticle colloidal suspension. It is detected that heat transmission rate is higher in $PEG + Cu_2O + MgO$ Hybrid nanofluid compared with $PEG + Graphene + Cu + Ag$ Hybrid nanofluid. For cooling purpose one can adopt PEG+ $Cu_2O + MgO$ hybrid nanofluid.

Keywords: phase change materials; Polyethylene glycol; Hybrid nanofluid; axisymmetric flow; heat transfer
Mathematics Subject Classification: 76-10, 76R10

1. Introduction

Phase change materials (recognized as PCMs) are functional materials which are recycled in several applications, for example in thermal energy storage, automotive industry, solar application, buildings, spacecraft thermal control applications etc. Usually, PCMs display high latent heat at melting temperatures, thermal/biochemical stabilities, low thermal conductivities and low toxicity. Recent studies [1–5] exposed that the thermal conductivity of base fluids of PCMs could be increased with the addition of solid particles (1 to 100 nm sized metals/ oxide/ carbon nanotubes carbide particles). Phase change materials encapsulated with nanoparticles enhanced the performance of the fluid as well as assisted in maintaining the device at an appropriate cooling temperature. Polyethylene glycol are semi- crystalline polymers deliberated as phase transformation materials (PCMs) it has extensive applications in medicine, lubricator, anti-fizzing agent in many foodstuff and drink products, in peel emulsions, toothpaste, technical ceramics, as an insulator and industrial manufacturing. PEG discloses great concealed heat storage aptitudes at the melting point temperatures which can be attuned via mutable the molecular form of the polymer. To enhance the thermal conductivity and heat transmission performance nanoparticles are mixed to PEG. PEG based nanofluid prevents both coagulation and agglomeration see Sahoo et al. [6]. Thermo physical properties of PEG with different nanoparticles are investigated by [7–10].

The interest towards dissolving nanoparticles in conventional heat transfer fluid is not a novel impression, any longer. Yet, the work is motivating and inspiring even though new fluids are convoluted. In current period, researchers technologically invented special class of heat transfer fluid known as Hybrid nanofluid. Hybrid nanofluid is the fluid comprising two or more than two types of nanoparticles with the conventional working fluid. Recently upadhya et al. [11] took up comparative analysis of hybrid nanofluid flow over curved stretching surface and noticed that micro polar fluid exhibit advanced entropy generation associated with Casson mixture nanofluid. Kumar et al. [12] explicated quadratic and linear convection in 3D hybrid nanofluid flow. Shah et al. [13] reported temperature and velocity distributions are declining with response to the improvement in second grade parameter in assisting and opposing flow. Ramesh et al. [14] examined ternary nanofluid flow through slipped surface and found that upgrading the suction parameter resulted in temperature

decline. Saleem et al. [15] studied hybrid nanofluid flow on a horizontal surface and witnessed that higher the density of spherical nanoparticles then lower will be the friction between the layers of fluid and the wall. Shah et al. [16] analyzed entropy optimization in hybrid nanofluid flow over a curved surface and observed entropy rate could be improved via strengthening the porosity variable. Mahesh et al. [17] explicated PEG based hybrid nanofluid flow and non-Fourier heat flux influence on entropy generation. By observing running industrial procedures in gas turbine engines, centrifuges, space crafts, ship propellers, turbo machinery, combustion chambers, heat exchangers, viscometers, centrifugal machines, calcination of cement, dryers and separators, automobile brakes and gear etc. engineers and researchers [18–22] in current days are convinced that flow induced through rotating objects possesses massive practical applications hence a profound study in this area is essential.

Studies associated with the fluid motion confined to the cylinder rotation and axial symmetry has contributed towards the advancement in sophisticated equipment with upgraded efficiency in nuclear reactor fuel rods, pipeline systems, heat exchangers, solar energy conversion devices, rocket motors, surgical instruments, crystal growth, drilling process, turbo machinery, electronic cooling, material processing systems, aviation for lift generation, axles and shafts toward spinning projectiles (as depicted in Figure 1) etc. First ever Crane [23] analyzed the two-dimensional flow persuaded by stretching cylinder. Ishak et al. [24] investigated influence of magnetic parameter, Reynolds number and Prandtl number on MHD movement over a widening cylinder. Javed et al. [25] analyzed axisymmetric Casson fluid flow through swirling cylinder and noted magnitude in axial friction enhancing for greater Reynold and magnetic parameter. Sarfraz et al. [26] analyzed consequences of Cattaneo-Christov on heat transport in swirling flow on a rotating cylinder. Khan et al. [27] studied impact of viscous dissipation on CNT nanofluid flow over rotating cylinder. Moayedi [28] analyzed and described nanofluid movement in a revolving cylinder in a cavity with the multiple ports. The interaction within electrically steering fluids and a magnetic flow (magneto hydrodynamic) is constantly considered by researchers in relative to pumps, hydro magnetic generator, meters, boundary layer control, etc. Hydro-magnetic boundary layers are experiential in several technical systems engaging plasma flows, induction flow meter and liquid metal in which flow directly depend on the potential differences within the fluid in perpendicular direction towards the motion and magnetic fields. Recently, researchers [29–35] investigated influence of magnetic field on the flow and heat transmission of an incompressible viscous hybrid/nanofluid past a stretching or rotating surface in a quiescent fluid.

Through the literature survey it is observed that research in new class of Polyethylene glycol (PEG) based nanofluid is in its pioneering phase. Thus, in this study we studied axisymmetric magneto hydrodynamic Polyethylene glycol (PEG) based hybrid nanofluid flow induced by a swirling cylinder. Flow and heat transfer is analyzed and compared for PEG+ Cu_2O + MgO and PEG+Graphene+ Cu + Ag hybrid nanofluid flow. Shooting procedure is imposed to work out the governing flow system. Simulated results are displayed through graphs. The computational results are validated with the published research work and established a modest coincidence.

2. Problem formulation

In this, considered the axisymmetric movement of hybrid nanofluid in an impermeable broadening and torsional indication of cylinder. The magnetic field also included in this investigation.

The induced magnetic field is abandoned due to low Reynolds number. The impact of swirling nature neglected the radiation and dissipative phenomena. The temperature is varying linearly stretching surface with axial distance of cylinder (see Figures 1 and 2).

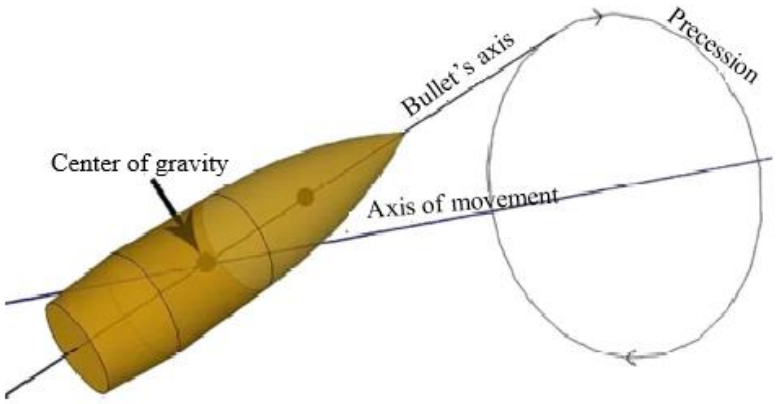

Figure 1. Spinning projectile.

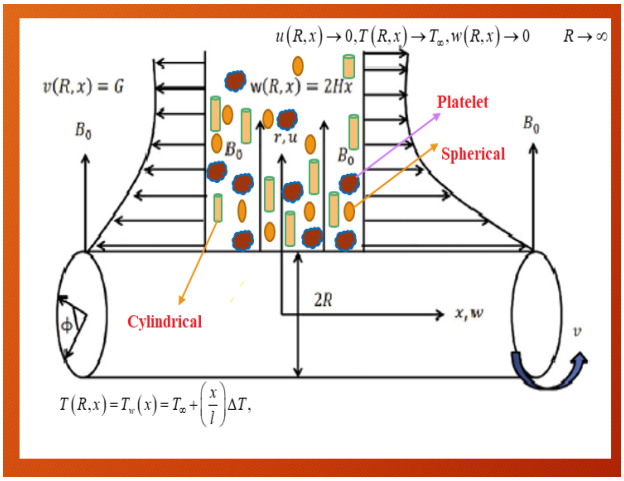

Figure 2. Physical model of the flow problem.

Current flow circumstances are governed by the succeeding equations (following Javed et al. [25]).

$$\frac{\partial u}{\partial r}+\frac{\partial w}{\partial x}=-\frac{u}{r}, \tag{1}$$

$$\rho_{hnf}\left(u\frac{\partial u}{\partial r}+w\frac{\partial u}{\partial x}-\frac{v^2}{r}\right)=-\frac{\partial p}{\partial r}+\mu_{hnf}\left(\frac{\partial^2 u}{\partial r^2}+\frac{1}{r}\frac{\partial u}{\partial r}+\frac{\partial^2 u}{\partial x^2}-\frac{u}{r^2}\right), \tag{2}$$

$$\rho_{hnf}\left(u\frac{\partial v}{\partial r}+w\frac{\partial v}{\partial x}+\frac{uv}{r}\right)=\mu_{hnf}\left(\frac{\partial^2 v}{\partial r^2}+\frac{1}{r}\frac{\partial v}{\partial r}+\frac{\partial^2 v}{\partial x^2}-\frac{v}{r^2}\right)-\sigma B_0^2 v, \tag{3}$$

$$\rho_{hnf}\left(u\frac{\partial w}{\partial r}+w\frac{\partial w}{\partial x}\right)=-\frac{\partial p}{\partial r}+\mu_{hnf}\left(\frac{\partial^2 w}{\partial r^2}+\frac{1}{r}\frac{\partial w}{\partial r}+\frac{\partial^2 w}{\partial x^2}\right)-\sigma B_0^2 w, \tag{4}$$

$$\left(\rho c_p\right)_{hnf}\left(u\frac{\partial T}{\partial r}+w\frac{\partial T}{\partial x}\right)=k_{hnf}\left(\frac{\partial^2 T}{\partial r^2}+\frac{1}{r}\frac{\partial T}{\partial r}+\frac{\partial^2 T}{\partial x^2}\right), \tag{5}$$

with corresponding boundaries are

$$\begin{aligned} &u\left(R,x\right)=0,\ T\left(R,x\right)=T_w\left(x\right)=T_\infty+\left(\frac{x}{l}\right)\Delta T, w\left(R,x\right)=2Hx,\ v\left(R,x\right)=G,\\ &u\left(R,x\right)\to 0, T\left(R,x\right)\to T_\infty, w\left(R,x\right)\to 0 \qquad R\to\infty \end{aligned} \tag{6}$$

where φ_1,φ_2 and φ_3 signifies volume of spherical (SS), Cylindrical (CS) and platelet(PS) nano particles. $\varphi=\varphi_1+\varphi_2+\varphi_3$ characterizes overall volume fraction of nanoparticles. The ternary mixture (SS, CS and PS shape of nanoparticles) viscosity and thermal conductivity are given by (Dinesh Kumar et al. [12]).

$$\mu_{hnf}=\varphi^{-1}(\mu_{nf1}\varphi_1+\mu_{nf2}\varphi_2+\mu_{nf3}\varphi_3), \tag{7}$$

$$k_{hnf}=\varphi^{-1}(k_{nf1}\varphi_1+k_{nf2}\varphi_2+k_{nf3}\varphi_3). \tag{8}$$

The density $\left(\rho_{hnf}\right)$ of ternary mixture (SS, CS and PS shape of nanoparticles) is given by (Dinesh Kumar et al. [12]).

$$\rho_{hnf}=(1-\varphi_1-\varphi_2-\varphi_3)\rho_{bf}+\varphi_1\rho_{sp1}+\varphi_2\rho_{sp2}+\varphi_3\rho_{sp3}, \tag{9}$$

$$\left(\rho\beta_0\right)_{hnf}=(1-\varphi_1-\varphi_2-\varphi_3)\left(\rho\beta_0\right)_{bf}+\varphi_1\left(\rho\beta_0\right)_{sp1}+\varphi_2\left(\rho\beta_0\right)_{sp2}+\varphi_3\left(\rho\beta_0\right)_{sp3}, \tag{10}$$

$$\left(\rho\beta_1\right)_{hnf}=(1-\varphi_1-\varphi_2-\varphi_3)\left(\rho\beta_1\right)_{bf}+\varphi_1\left(\rho\beta_1\right)_{sp1}+\varphi_2\left(\rho\beta_1\right)_{sp2}+\varphi_3\left(\rho\beta_1\right)_{sp3}. \tag{11}$$

The heat capacity $(\rho c_p)_{hnf}$ of ternary mixture (SS, CS and PS shape of nanoparticles) is given by (Dinesh Kumar et al. [12]).

$$(\rho c_p)_{hnf}=(1-\varphi_1-\varphi_2-\varphi_3)(\rho c_p)_{bf}+\varphi_1(\rho c_p)_{sp1}+\varphi_2(\rho c_p)_{sp2}+\varphi_3(\rho c_p)_{sp3}. \tag{12}$$

Viscosity and thermal conductivity for spherical (SS) nanoparticles is: (Dinesh Kumar et al. [12]).

$$\mu_{nf1}=\left(\mu_{bf}\right)\left(1+2.5\varphi+6.2\varphi^2\right), \tag{13}$$

$$\frac{k_{nf1}}{k_{bf}} = \left[\frac{k_{sp1} + 2k_{bf} - 2\varphi(k_{bf} - k_{sp1})}{k_{sp1} + 2k_{bf} + \varphi(k_{bf} - k_{sp1})} \right]. \tag{14}$$

Thermal conductivity and viscosity for cylindrical (CS) nanoparticles is: (Dinesh Kumar et al. [12]).

$$\frac{\mu_{nf2}}{\mu_{bf}} = \left(1 + 13.5\varphi + 904.4\varphi^2\right), \tag{15}$$

$$\frac{k_{nf2}}{k_{bf}} = \left[\frac{k_{sp2} + 3.9k_{bf} - 3.9\varphi(k_{bf} - k_{sp2})}{k_{sp2} + 3.9k_{bf} + \varphi(k_{bf} - k_{sp2})} \right]. \tag{16}$$

Thermal conductivity and viscosity for platelet (PS) nanoparticles is: (Dinesh Kumar et al. [12]).

$$\frac{\mu_{nf3}}{\mu_{bf}} = \left(1 + 37.1\varphi + 612.6\varphi^2\right), \tag{17}$$

$$\frac{k_{nf3}}{k_{bf}} = \left[\frac{k_{sp3} + 4.7k_{bf} - 4.7\varphi(k_{bf} - k_{sp3})}{k_{sp3} + 4.7k_{bf} + \varphi(k_{bf} - k_{sp3})} \right]. \tag{18}$$

Applying

$$\begin{aligned} &\eta = \left(\frac{r^2}{R^2}\right), \qquad \frac{u}{HR} = -\frac{f(\eta)}{\sqrt{\eta}}, \; v = Gg(\eta), \\ &w = 2Hxf'(\eta), \qquad \theta(\eta) = \frac{T - T_\infty}{T_w - T_\infty} \end{aligned} . \tag{19}$$

The continuity is satisfied identically and rest of the terminologies (i.e. (2)–(6)) has the absolute forms:

$$\frac{A_1}{A_2\phi}\left(\eta f''' + f''\right) - Mf' + \mathrm{Re}\left(ff'' - f'^2\right) = 0, \tag{20}$$

$$\frac{A_1}{A_2\phi}\left(\eta g'' + g' - \frac{g}{4\eta}\right) + \mathrm{Re}\left(fg' - \frac{fg}{2\eta}\right) - Mg = 0, \tag{21}$$

$$\frac{A_3}{\phi}\eta\theta'' + \theta' + A_4 \,\mathrm{Pr}\,\mathrm{Re}\left(f\theta' - f'\theta\right) = 0, \tag{22}$$

$$\begin{aligned} &f(1) = 0, f'(1) = 1, g(1) = 1, \theta(1) = 1, \\ &f'(\infty) \to 0, \theta(\infty) \to 0, g(\infty) \to 0. \end{aligned} \tag{23}$$

In the above equations,

$$A_1 = B_1\varphi_1 + B_2\varphi_2 + B_3\varphi_3,$$

$$A_2 = 1-\varphi_1-\varphi_2-\varphi_3+\varphi_1\frac{\rho_{sp1}}{\rho_{bf}}+\varphi_2\frac{\rho_{sp2}}{\rho_{bf}}+\varphi_3\frac{\rho_{sp3}}{\rho_{bf}},$$

$$A_3 = B_4\varphi_1 + B_5\varphi_2 + B_6\varphi_3,$$

$$A_4 = 1-\varphi_1-\varphi_2-\varphi_3+\varphi_1\frac{(\rho c_p)_{sp1}}{(\rho c_p)_{bf}}+\varphi_2\frac{(\rho c_p)_{sp2}}{(\rho c_p)_{bf}}+\varphi_3\frac{(\rho c_p)_{sp3}}{(\rho c_p)_{bf}},$$

$$A_5 = \left(1-\varphi_1-\varphi_2-\varphi_3\right)+\varphi_1\frac{\left(\rho\beta_0\right)_{sp1}}{\left(\rho\beta_0\right)_{bf}}+\varphi_2\frac{\left(\rho\beta_0\right)_{sp2}}{\left(\rho\beta_0\right)_{bf}}+\varphi_3\frac{\left(\rho\beta_0\right)_{sp3}}{\left(\rho\beta_0\right)_{bf}},$$

$$A_6 = \left(1-\varphi_1-\varphi_2-\varphi_3\right)+\varphi_1\frac{\left(\rho\beta_1\right)_{sp1}}{\left(\rho\beta_1\right)_{bf}}+\varphi_2\frac{\left(\rho\beta_1\right)_{sp2}}{\left(\rho\beta_1\right)_{bf}}+\varphi_3\frac{\left(\rho\beta_1\right)_{sp3}}{\left(\rho\beta_1\right)_{bf}},$$

$$B_1 = 1+2.5\varphi+6.2\varphi^2,$$

$$B_2 = 1+13.5\varphi+904.4\varphi^2,$$

$$B_3 = 1+37.1\varphi+612.6\varphi^2,$$

$$B_4 = \frac{k_{sp1}+2k_{bf}-2\varphi(k_{bf}-k_{sp1})}{k_{sp1}+2k_{bf}+\varphi(k_{bf}-k_{sp1})},$$

$$B_5 = \frac{k_{sp2}+3.9k_{bf}-3.9\varphi(k_{bf}-k_{sp2})}{k_{sp2}+3.9k_{bf}+\varphi(k_{bf}-k_{sp2})},$$

$$B_6 = \frac{k_{sp3}+4.7k_{bf}-4.7\varphi(k_{bf}-k_{sp3})}{k_{sp3}+4.7k_{bf}+\varphi(k_{bf}-k_{sp3})}.$$

The involved physical effects in flow problem have the succeeding descriptions

$$Re = \frac{HR^2}{2v}, M = \frac{\sigma B_0^2 R^2}{4v\rho}, Pr = \frac{v}{\alpha}. \tag{24}$$

Reynolds number Re, Prandtl number Pr, magnetic parameter M.

The physical magnitudes of manufacturing viewpoint the friction factor $\left(C_{fx}\ and\ C_{f\phi}\right)$ quantities and Nusselt number $\left(Nu_x\right)$ are

$$C_{fx}\left(\frac{x}{R}\right)=\mathrm{Re}^{-1}\frac{A_1}{\phi}\,f''(1), \tag{25}$$

$$C_{f\phi}\,\mathrm{Re}\left(\frac{G}{HR}\right)=\frac{A_1}{\phi}\left[2g'(1)-g(1)\right], \tag{26}$$

$$\frac{Nu}{2}=-\frac{A_3}{\phi}\theta'(1). \tag{27}$$

3. Interpretation of results and discussion

The nonlinear ODEs. (20)–(22) with well-defined boundary circumstance (23) is elucidated numerically by R-K based shooting technique with help of MATLAB software. The influence of Reynolds number Re, magnetic M, Volume fraction of concentration ϕ, on axial velocity $f'(\eta)$, swirl velocity $g(\eta)$, radial velocity $f(\eta)/\eta^{0.5}$, temperature $\theta(\zeta)$, surface drag force $C_{fx}\,\mathrm{Re}\left(\frac{x}{R}\right)$, $C_{f\phi}\,\mathrm{Re}\left(\frac{G}{HR}\right)$ and heat transfer rate $\theta'(1)$ are discussed through preparation of graphs (Figures 3-23). The convergence series of the dimensionless factors are agreed as $\mathrm{Re}\in[1,2,3]$, $M\in[0.5,1,1.5]$. $\phi\in[0.01,0.03,0.05]$.

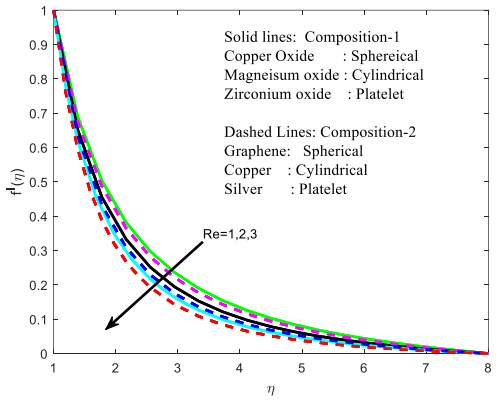

Figure 3. Re variation on $f'(\eta)$.

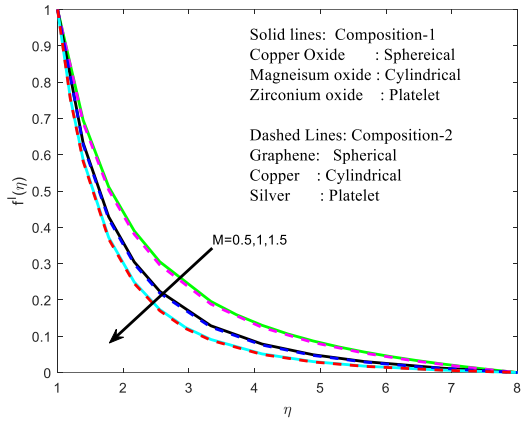

Figure 4. M variation on $f'(\eta)$.

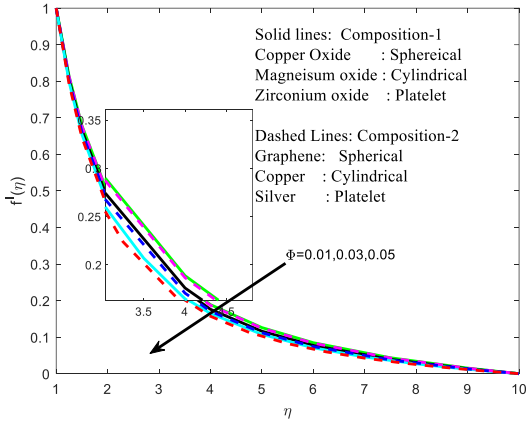

Figure 5. ϕ variation on $f'(\eta)$.

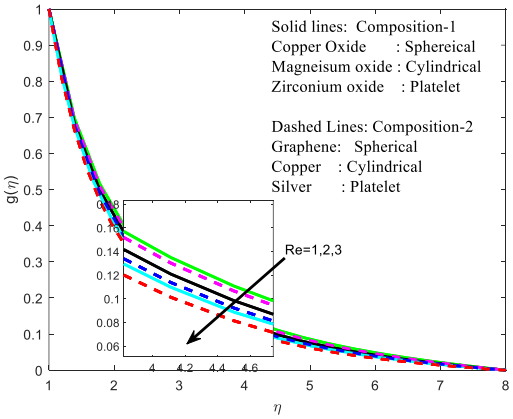

Figure 6. Re variation on $g(\eta)$.

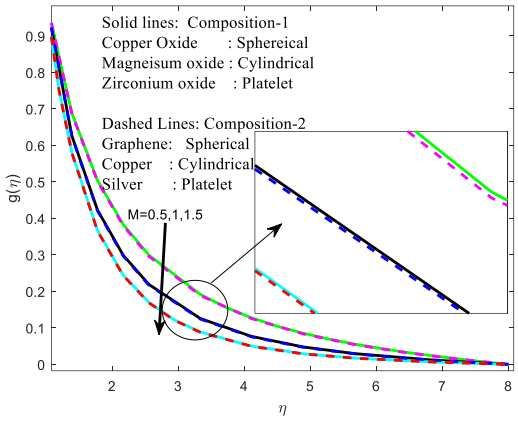

Figure 7. M variation on $g(\eta)$.

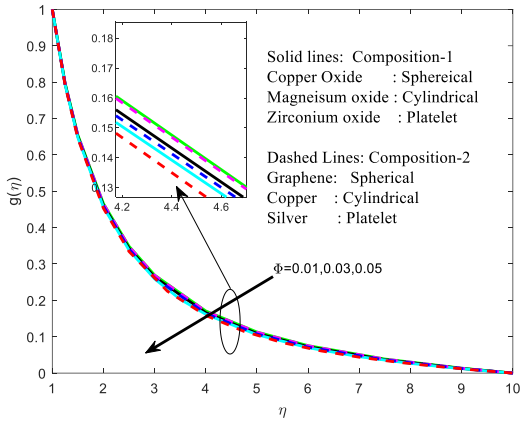

Figure 8. ϕ variation on $g(\eta)$.

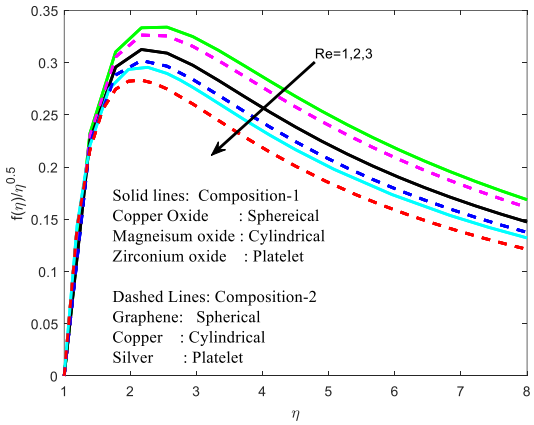

Figure 9. Re variation on $f(\eta)/\eta^{0.5}$.

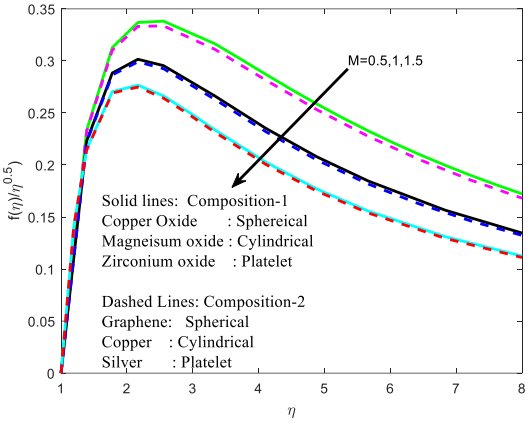

Figure 10. M variation on $f(\eta)/\eta^{0.5}$.

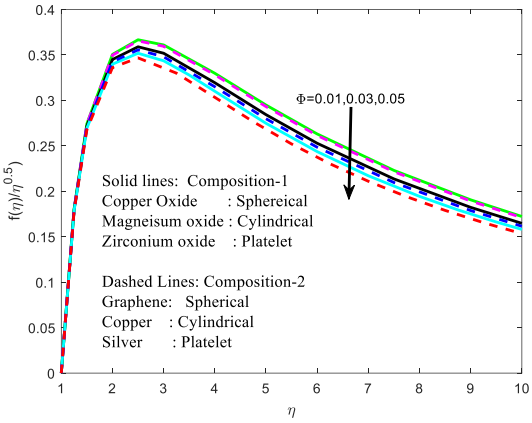

Figure 11. ϕ variation on $f(\eta)/\eta^{0.5}$.

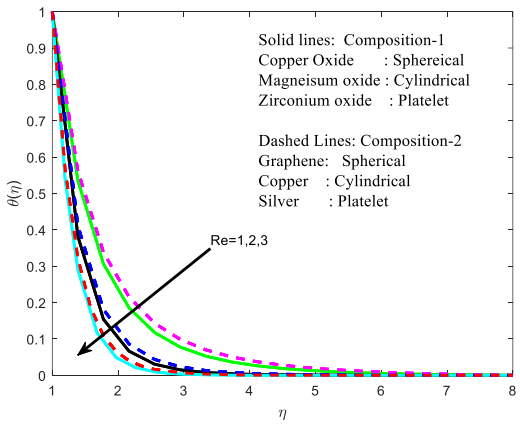

Figure 12. Re variation on $\theta(\eta)$.

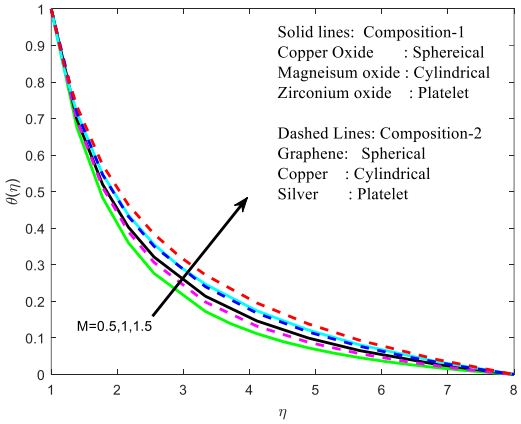

Figure 13. M variation on $\theta(\eta)$.

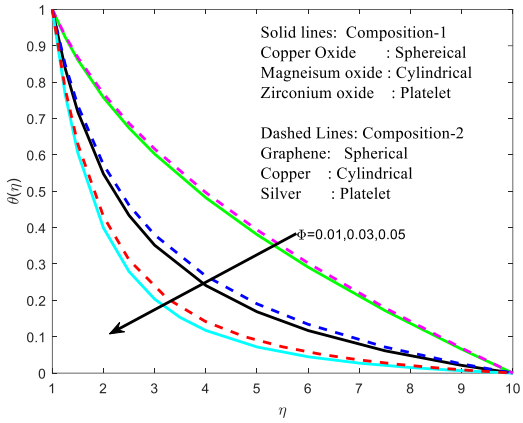

Figure 14. ϕ variation on $\theta(\eta)$.

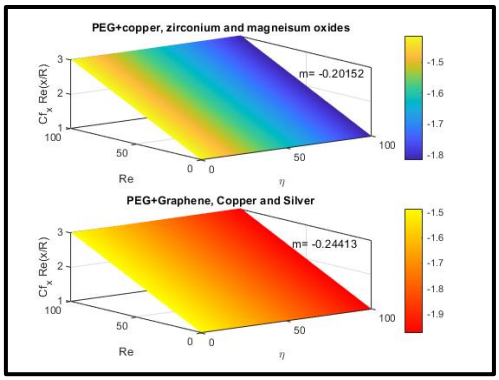

Figure 15. Influence of Re on surface drag force $C_{fx}\,\mathrm{Re}\left(\frac{x}{R}\right)$.

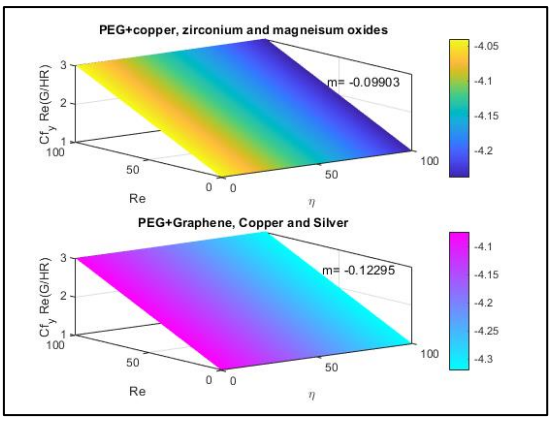

Figure 16. Influence of Re on surface drag force $C_{f\phi}\,\mathrm{Re}\left(\frac{G}{HR}\right)$.

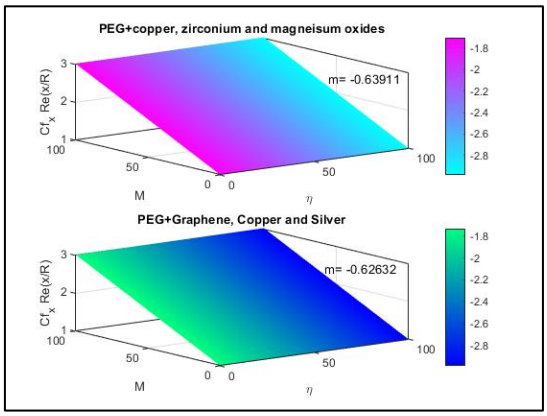

Figure 17. Influence of M on surface drag force $C_{fx}\,\mathrm{Re}\left(\frac{x}{R}\right)$.

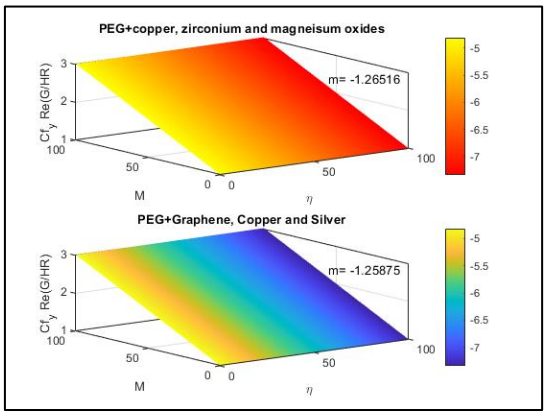

Figure 18. Influence of Re on surface drag force $C_{f\phi}\,\mathrm{Re}\left(\frac{G}{HR}\right)$.

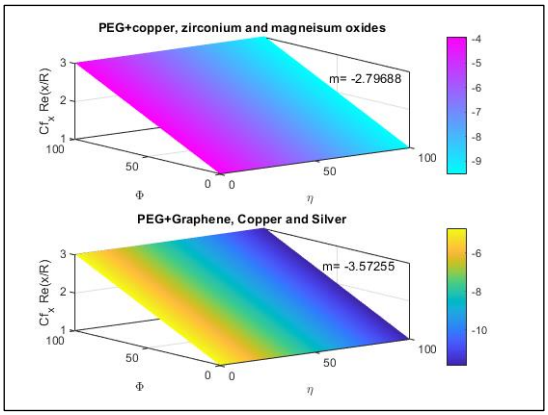

Figure 19. Influence of ϕ on surface drag force $C_{fx}\,\mathrm{Re}\left(\frac{x}{R}\right)$.

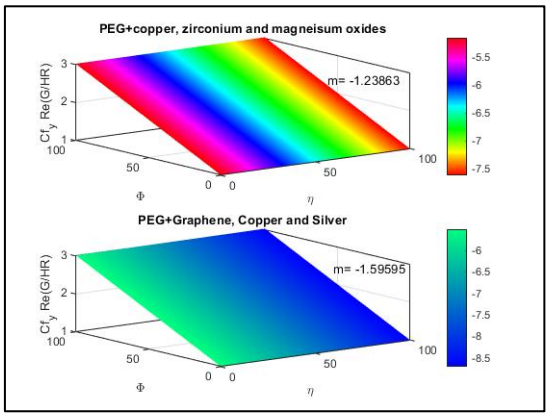

Figure 20. Influence of ϕ on surface drag force $C_{f\phi}\,\mathrm{Re}\left(\frac{G}{HR}\right)$.

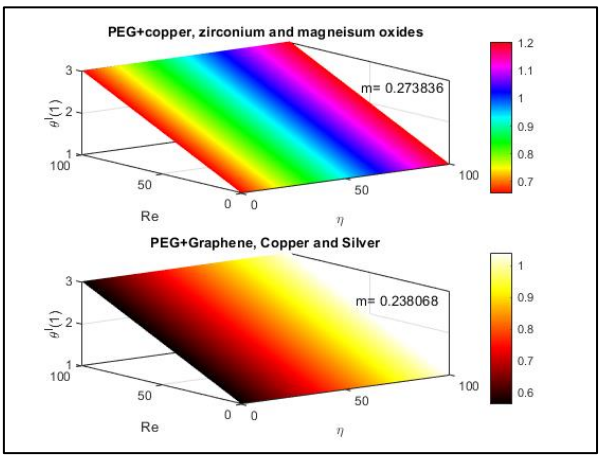

Figure 21. Influence of Re on heat transfer rate.

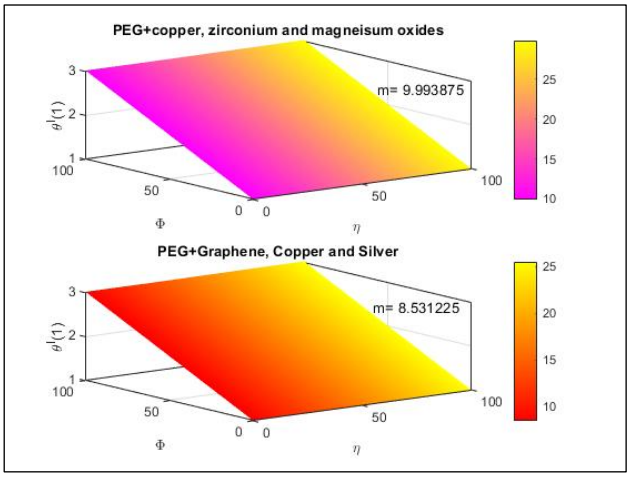

Figure 22. Influence of ϕ on heat transfer rate.

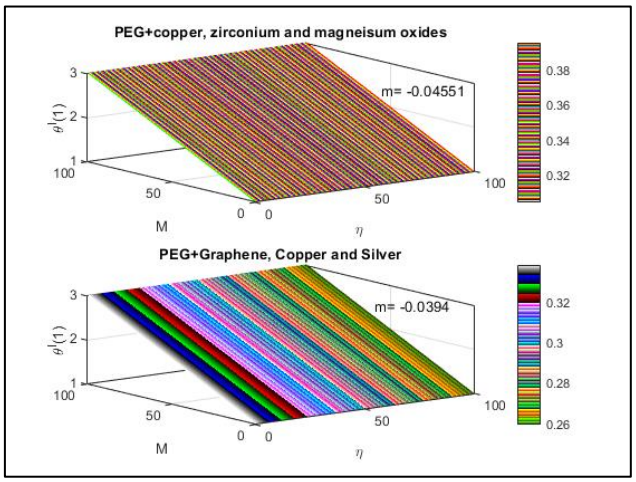

Figure 23. Influence of M on heat transfer rate.

Flow and heat transfer is analyzed and compared for PEG+Cu_2O+MgO and PEG+Graphene+$Cu+Ag$ hybrid nanofluid flow. In the figure solid lines indicates Polyethylene glycol based copper oxide, magnesium oxide and zirconium oxide hybrid nanofluid (PEG+Cu_2O+MgO)and dashed lines indicate Polyethylene glycol based Graphene, copper and silver hybrid nanofluid (PEG+Graphene+$Cu+Ag$). Copper oxide (Cu_2O), Magnesium oxide (MgO), zirconium oxide (ZrO_2), Graphene, Copper(Cu), Silver(Ag) at 25 °C applied for simulation of the outcomes are itemized in Table 1. The current solutions are authenticated with available information in limiting method (see Table 2) and initiated to be equitable.

Table 1. Thermo physical properties of base fluid polyethylene glycol (PEG), nanoparticles Copper oxide Magnesium oxide (MgO), zirconium oxide (ZrO_2), Graphene, Copper (Cu), Silver (Ag).

Thermo physical properties	polyethylene glycol (PEG)	Copper oxide (Cu_2O)	Magnesium oxide (MgO)	zirconium oxide (ZrO_2)	Graphene	Copper (Cu)	Silver (Ag)
$\rho\left(Kgm^{-3}\right)$	1110	6500	3560	5680	2200	8933	10500
$c_p\left(Jkg^{-1}K^{-1}\right)$	3354	535.6	955	502	790	385	235
$k\left(Wm^{-1}K^{-1}\right)$	0.3712	20	45	1.7	5000	400	429
Prandtl number	2	-	-	-			

Table 2. Comparison of $f''(\eta=1)$ with reference to the available literature for varying values of M and Re considering $A_1=A_2=A_3=\phi=\beta=Q_0=0$.

	Re =1			Re =5		
M	Present	Javed et al. [25]	Ishak et al. [24]	Present	Javed et al. [25]	Ishak et al. [24]
0	-1.1785	-1.1784	-1.1780	-2.4174	-2.4173	-2.4174
0.01	-1.1842	-1.1842	-1.1839	-2.4199	-2.4198	-2.4199
0.05	-1.2072	-1.2070	-1.2068	-2.4294	-2.4295	-2.4296
0.1	-1.2345	-1.2344	-1.2344	-2.4417	-2.4416	-2.4417
0.5	-1.4270	-1.4269	-1.4269	-2.5353	-2.5351	-2.5352

Reynolds number (Re) denotes ratio between inertial force and viscous force. Re exhibits prominent part in anticipating design in hybrid nano fluid performance which is generated by wall stretching owing to the viscous forces. Variation in large Re specifies the flow as turbulent while the smaller variations in Re signifies flow to be laminar. Diminishing Re $(\mathrm{Re}=0)$ postulates swirl velocity $(g(\eta))$ is independent of axial velocity $(f'(\eta))$. Non zero Reynolds number Re $(\mathrm{Re}\neq 0)$ illustrate that hybrid nanofluid motion is influenced by the torsional motion. In this study, flow is considered to be laminar. Fig. 3, 4 and 5 portray the influence of improving Reynolds number Re, Volume fraction of nanoparticles concentration ϕ, magnetic M, on axial velocity $(f'(\eta))$. Through Figure 3 it is noted that larger values of Re develop more inertial force among the fluid particles hence causes decay in axial velocity. Also, it is noticed that axial velocity is more decaying in PEG+Graphene+ $Cu+Ag$ than in PEG+ Cu_2O+MgO. It is important to observe the behavior of Re towards nanoparticles suspension platelet shaped nanoparticle colloidal suspension exhibit more decaying axial velocity compared to spherical shaped nanoparticle colloidal suspension. Figure 4 illustrates the behavior in axial velocity for enlarging values of M. Greater values of M generates drag force on fluid atoms typically recognized as Lorentz force. This energy exhibits the propensity of slow down the fluid motion nearby rotating cylinder hence there is decrease in $f'(\eta)$. Similarly, it is observed that magnetic field lessens axial velocity in PEG+Graphene+ $Cu+Ag$ hybrid nanofluid compared to PEG+ Cu_2O+MgO hybrid nanofluid and platelet shaped nanoparticle colloidal

suspension exhibit more decaying axial velocity compared to spherical shaped nanoparticle colloidal suspension. In Figure 5 it is witnessed that more the concentration of nanoparticles lesser the axial velocity of rotating cylinder. Increment in ϕ lower the axial velocity of PEG+Graphene+ $Cu + Ag$ hybrid nanofluid compared to PEG+ $Cu_2O + MgO$.

Figures 6–8 reveal the behavior of $g(\eta)$ swirl velocity for Reynolds number Re, magnetic M, volume fraction of nanoparticles concentration ϕ. $g(\eta)$ deteriorates with enhancement of Re, M and ϕ. Improvement in Re boost the inertial force in hybrid nanofluid particles which reduces the fluid rotation. Application of M develops Lorentz force in hybrid nanofluid particles hence swirl velocity is reduced. Similarly, in Figure 8 it is observed more the volume fraction of nanoparticle lesser the swirl velocity. Through Figures 6–8 commonly it is experienced that swirl velocity of PEG+Graphene+ $Cu + Ag$ hybrid nanofluid decays more compared to PEG+ $Cu_2O + MgO$ hybrid nanofluid and platelet shaped nanoparticle colloidal suspension exhibit more decaying swirl velocity compared to spherical shaped nanoparticle colloidal suspension.

The analogous behavior is observed for the radial velocity $\left(f(\eta)/\eta^{0.5}\right)$, with discrepancy in Reynolds number Re, magnetic parameter M, volume fraction of concentration ϕ.Here $f(\eta)/\eta^{0.5}$ radial velocity achieves its supreme value near the rotating cylinder and $f(\eta)/\eta^{0.5}$ progressively decrease as revealed in the Figures 9–11.The radial velocity is induced because of cylinder wall elongating in axial direction. $f(\eta)/\eta^{0.5}$ for PEG+Graphene+ $Cu + Ag$ hybrid nanofluid decays more compared to PEG+ $Cu_2O + MgO$ hybrid nanofluid and platelet shaped nanoparticle colloidal suspension exhibit more decaying radial velocity compared to spherical shaped nanoparticle colloidal suspension.

Figures 12–14 depict the temperature field $\theta(\zeta)$ with regard to variations in Reynolds number Re, magnetic M, volume fraction of nanoparticles concentration ϕ. Via Figure 12 it is perceived that development in Re declines the temperature of the hybrid nanofluid. In Figure 13 it is noted that improvement in M leads to rise in temperature of the hybrid nanofluid. With enhancement in M Lorentz force is developed in the hybrid nanofluid this opposes the movement in fluid particle as an outcome additional heat is developed hereafter temperature of the hybrid nanofluid upsurges. PEG+Graphene+ $Cu + Ag$ hybrid nanofluid flow displays greater temperature outline associated with PEG+ $Cu_2O + MgO$ hybrid nanofluid. In Figure 14 it is witnessed that enlargement in ϕ temperature of the fluid is decreased. Larger the concentration of nanoparticles thermal conductivity of fluid is decreased and hence thermal boundary layer due to rotating of the cylinder is decreased. Improvement in ϕ lowers temperature profile of PEG+ $Cu_2O + MgO$ hybrid nanofluid compared to PEG+Graphene+ $Cu + Ag$ hybrid nanofluid. Hence for cooling purpose one can adopt PEG+ $Cu_2O + MgO$ hybrid nanofluid.

Impact of physical variables Re, M, ϕ on the factors of axial drag force $C_{fx}\,\mathrm{Re}\left(R^{-1}x\right)$, and tangential drag force $C_{f\phi}\,\mathrm{Re}\left(G(HR)^{-1}\right)$ and heat transmission rate are depicted in through Figures 15–23. From Figures 15 and 16 it is witnessed that axial and tangential drag force decrease with the improvement in Re in PEG+ $Cu_2O + MgO$ and PEG+Graphene+ $Cu + Ag$ hybrid nanofluid flow. It is interesting to note that $C_{fx}\,\mathrm{Re}\left(R^{-1}x\right)$ and $C_{f\phi}\,\mathrm{Re}\left(G(HR)^{-1}\right)$ is higher in $PEG + Cu_2O + MgO$ Hybrid nanofluid compared with $PEG + Graphene + Cu + Ag$ Hybrid nanofluid. Through Figures 17

and 18 it is evident that improvement in M declines $C_{fx}\,\mathrm{Re}\left(R^{-1}x\right)$ and $C_{f\phi}\,\mathrm{Re}\left(G(HR)^{-1}\right)$ in PEG+ $Cu_2O + MgO$ and PEG+Graphene+ $Cu + Ag$ hybrid nanofluid flow. It is also observed that $C_{fx}\,\mathrm{Re}\left(R^{-1}x\right)$ and $C_{f\phi}\,\mathrm{Re}\left(G(HR)^{-1}\right)$ is higher in $PEG + Cu_2O + MgO$ Hybrid nanofluid compared with $PEG + Graphene + Cu + Ag$ Hybrid nanofluid. From Figures 19 and 20 it is evident that improvement in ϕ declines $C_{fx}\,\mathrm{Re}\left(R^{-1}x\right)$ and $C_{f\phi}\,\mathrm{Re}\left(G(HR)^{-1}\right)$ in PEG+ $Cu_2O + MgO$ and PEG+Graphene+ $Cu + Ag$ hybrid nanofluid flow. It is also observed that $C_{fx}\,\mathrm{Re}\left(R^{-1}x\right)$ and $C_{f\phi}\,\mathrm{Re}\left(G(HR)^{-1}\right)$ is higher in $PEG + Cu_2O + MgO$ Hybrid nanofluid compared with $PEG + Graphene + Cu + Ag$ Hybrid nanofluid.

From Figures 21 and 22 it is observed that Local Nusselt number is increasing function of Re and ϕ in hybrid nanofluid flow. From Figure 23 it is perceived that Nusselt number is declining function of M in hybrid nanofluid flow. Overall, it is detected that heat transmission rate is higher in $PEG + Cu_2O + MgO$ Hybrid nanofluid compared with $PEG + Graphene + Cu + Ag$ Hybrid nanofluid.

4. Concluding remarks

Polyethylene glycol (PEG) based magneto hydrodynamic hybrid nanofluid flow induced by a swirling cylinder is scrutinized numerically (shooting procedure, R-K 4th order based) in this investigation. Flow and heat transfer is explored and compared for PEG+ $Cu_2O + MgO$ and PEG+Graphene+ $Cu + Ag$ hybrid nanofluid flow. Following are the foremost outcome of this study:

- The axial, swirl and radial velocities in hybrid nanofluid are observed to decay with improvement in Reynolds number, nanofluid volume fraction and magnetic parameter.
- Platelet shaped nanoparticle colloidal suspension exhibit more decaying axial, swirl and radial velocity compared to spherical shaped nanoparticle colloidal suspension.
- Temperature of hybrid nanofluid observed to decline against the larger values of Reynolds number and nanofluid volume fraction.
- Temperature field is increasing function of magnetic parameter.
- Axial and tangential drag force decrease with the improvement in Reynolds number, magnetic parameter and nanoparticle volume fraction in PEG+ $Cu_2O + MgO$ and PEG+Graphene+ $Cu + Ag$ hybrid nanofluid flow.
- Heat transfer rate improves with improvement in Reynolds number and nanoparticle volume fraction decays for magnetic parameter.

Limitations:

(1) The Reynolds number is low due to this induced magnetic field is neglected.

(2) The viscous dissipation and internal heat generation/absorption is neglected.

(3) The impacts of linear and nonlinear buoyancy forces as well as thermal radiation is neglected.

(4) The present considered study is incompressible, laminar and steady case. Also non-uniform heat source or sink not considered due to rotation.

Abbreviation:

Spherical shape: SS, Cylindrical Shape: CS, Platelet Shape: PS, PEG: Propylene Ethylene Glycol, Copper oxide: Cu_2O, Magnesium oxide: MgO, zirconium oxide: ZrO_2, Copper: Cu, Silver: Ag.

Acknowledgements

This research received funding support from the NSRF via the Program Management Unit for Human Resources & Institutional Development, Research and Innovation, (grant number B05F650018).

Conflict of interest

The authors declare no conflicts of interest.

References

1. P. M. Kumar, D. Sudarvizhi, P. M. J. Stalin, A. Aarif, R. Abhinandhana, A. Renuprasanth, N. et al., Thermal characteristics analysis of a phase change material under the influence of nanoparticles, *Mater. Today: P.*, **45** (2021), 7876–7880. https://doi.org/10.1016/j.matpr.2020.12.505
2. O. K. Koriko, K. S. Adegbie, I. L. Animasaun, M. A. Olotu, Numerical solutions of the partial differential equations for investigating the significance of partial slip due to lateral velocity and viscous dissipation: the case of blood-gold Carreau nanofluid and dusty fluid, *Numer. Methods Part. Differ. Equ.*, **7** (2021), 1–15. https://doi.org/10.1002/num.22754
3. H. Faraji, M. El Alami, A. Arshad, Investigating the effect of single and hybrid nanoparticles on melting of phase change material in a rectangular enclosure with finite heat source, *Int. J. Energ. Res.*, **45** (2021), 4314–4330. https://doi.org/10.1002/er.6095
4. A. N. Sadr, M. Shekaramiz, M. Zarinfar, A. Esmaily, H. Khoshtarash, D. Toghraie, Simulation of mixed-convection of water and nano-encapsulated phase change material inside a square cavity with a rotating hot cylinder, *J. Energy Storage*, **47** (2022), 103606. https://doi.org/10.1016/j.est.2021.103606
5. N. A. Shah, A. Wakif, E. R. El-Zahar, T. Thumma, S.-J. Yook, Heat transfers thermodynamic activity of a second-grade ternary nanofluid flow over a vertical plate with Atangana-Baleanu time-fractional integral, *Alexandria Eng. J.*, **61** (2022), 10045–10053. https://doi.org/10.1016/j.aej.2022.03.048
6. R. K. Sahu, S. H. Somashekhar, P. V. Manivannan, Investigation on copper nanofluid obtained through micro electrical discharge machining for dispersion stability and thermal conductivity, *Procedia Eng.*, **64** (2013), 946–955. https://doi.org/10.1016/j.proeng.2013.09.171
7. X. Zhang, Z. Huang, B. Ma, R. Wen, X. Min, Y. Huang, et al., Preparation and performance of novel form-stable composite phase change materials based on polyethylene glycol/white carbon black assisted by superultrasound-assisted, *Thermochim. Acta.*, **638** (2016), 35–43. https://doi.org/10.1016/j.tca.2016.06.012
8. D. Cabaleiro, S. Hamze, J. Fal, M. A. Marcos, P. Estell´e, G. Zyła, Thermal and physical characterization of PEG phase change materials enhanced by carbon-based nanoparticles, *Nanomaterials*, **10** (2020), 1168.
9. M. A. Marcos, D. Cabaleiro, M. J .G. Guimarey, M. J. P. Comu˜nas, L. Fedele, J. Fern´andez, et al., PEG 400-based phase change materials nano-enhanced with functionalized graphene nanoplatelets, *Nanomaterials*, **8** (2018), 16.

10. S. M. Upadhya, C. S. K. Raju, K. Vajravelu, S. Sathy, U. Farooq, Significance of radiative magnetohydrodynamic flow of suspended PEG based ZrO2 and MgO2 within a conical gap, *Wave. Random Complex*, 2022, 1–19. https://doi.org/10.1080/17455030.2021.2020372
11. S. M. Upadhya, S. S. R. Raju, C. S. K. Raju, N. A. Shah, J. D. Chung, Importance of entropy generation on Casson, Micropolar and Hybrid magneto-nanofluids in a suspension of cross diffusion, *Chinese J. Phys.*, **77** (2022), 1080–1101. https://doi.org/10.1016/j.cjph.2021.10.016
12. M. Dinesh Kumar, C. S. K. Raju, K. Sajjan, E. R. El-Zahar, N. A. Shah, Linear and quadratic convection on 3D flow with transpiration and hybrid nanoparticles, *Int. Commun. Heat Mass*, **134** (2022), 105995. https://doi.org/10.1016/j.icheatmasstransfer.2022.105995
13. N. A. Shah, S. J. Yook, O. Tosin, Analytic simulation of thermophoretic second grade fluid flow past a vertical surface with variable fluid characteristics and convective heating, *Sci. Rep.*, **12** (2022), 1–17. https://doi.org/10.1038/s41598-022-09301-x
14. G. K. Ramesh, J. K. Madhukesh, R. Das, N. A. Shah, S. J. Yook, Thermodynamic activity of a ternary nanofluid flow passing through a permeable slipped surface with heat source and sink, *Wave. Random Complex*, 2022, 1–21. https://doi.org/10.1080/17455030.2022.2053237
15. S. Saleem, I. L. Animasaun, S. J. Yook, Q. M. Al-Mdallal, N. A. Shah, M. Faisal, Insight into the motion of water conveying three kinds of nanoparticles on a horizontal surface: significance of thermo-migration and Brownian motion of different nanoparticles, *Surf. Interfaces*, **30** (2022), 101854. https://doi.org/10.1016/j.surfin.2022.101854
16. F. Shah, S. A. Khan, K. Al-Khaled, M. I. Khan, S. U. Khan, N. A. Shah, et al., Impact of entropy optimized Darcy-Forchheimer flow in MnZnFe2O4 and NiZnFe2O4 hybrid nanofluid towards a curved surface, *ZAMM J. Appl. Math. Mech.*, **102** (2022), e202100194. https://doi.org/10.1002/zamm.202100194
17. A. Mahesh, S. V. K. Varma, C. S. K. Raju, M. J. Babu, K. Vajravelu, W. Al-Kouz, Significance of non-Fourier heat flux and radiation on PEG–Water based hybrid Nanofluid flow among revolving disks with chemical reaction and entropy generation optimization, *Int. Commun. Heat Mass*, **127** (2021), 105572. https://doi.org/10.1016/j.icheatmasstransfer.2021.105572
18. H. P. Greenspan, *The theory of rotating fluids*, London: Cambridge University Press, 1968.
19. I. V. Shevchuk, *Modelling of convective heat and mass transfer in rotating flows*, New York: Springer, 2016.
20. S. S. K. Raju, M. J. Babu, C. S. K. Raju, Irreversibility analysis in hybrid nanofluid flow between two rotating disks with activation energy and cross-diffusion effects, *Chinese J. Phys.*, **72** (2021), 499–529. https://doi.org/10.1016/j.cjph.2021.03.016
21. B. Ali, Y. Nie, S. Hussain, D. Habib, S. Abdal, Insight into the dynamics of fluid conveying tiny particles over a rotating surface subject to Cattaneo–Christov heat transfer, Coriolis force, and Arrhenius activation energy, *Comput. Math. Appl.*, **93** (2021), 130–143. https://doi.org/10.1016/j.camwa.2021.04.006
22. S. M. Upadhya, R. L. V. Devi, C. S. K. Raju, H. M. Ali, Magnetohydrodynamic nonlinear thermal convection nanofluid flow over a radiated porous rotating disk with internal heating, *J. Therm. Anal. Calorim.*, **143** (2021), 1973–1984. https://doi.org/10.1007/s10973-020-09669-w
23. L. J. Crane, Boundary layer flow due to a stretching cylinder, *Z. Angew Math. Phy.*, **26** (1975), 619–622.

24. A. Ishak, R. Nazar, I. Pop, Magnetohydrodynamic (MHD) flow and heat transfer due to a stretching cylinder, *Energy Convers. Manage.*, **49** (2008), 3265–3269. https://doi.org/10.1016/j.enconman.2007.11.013
25. M. F. Javed, M. I. Khan, N. B. Khan, R. Muhammad, M. U. Rehman, S. W. Khan, et al., Axisymmetric flow of Casson fluid by a swirling cylinder, *Results Phys.*, **9** (2018), 1250–1255. https://doi.org/10.1016/j.rinp.2018.04.015
26. M. Sarfraz, A. Ahmed, M. Khan, M. M. Iqbal Ch, M. Azam, Significance of the Cattaneo–Christov theory for heat transport in swirling flow over a rotating cylinder, *Wave. Random Complex*, 2021, 1–13. https://doi.org/10.1080/17455030.2021.2015545
27. M. Khan, M. Sarfraz, A. Ahmed, M. Y. Malik, A. S. Alqahtani, Study of engine-oil based CNT nanofluid flow on a rotating cylinder with viscous dissipation, *Phys. Scr.*, **96** (2021), 075005. https://doi.org/10.1088/1402-4896/abfacd
28. H. Moayedi, Investigation of heat transfer enhancement of Cu-water nanofluid by different configurations of double rotating cylinders in a vented cavity with different inlet and outlet ports, *Int. Commun. Heat Mass*, **126** (2021), 105432. https://doi.org/10.1016/j.icheatmasstransfer.2021.105432
29. K. U. Rehman, W. Shatanawi, Q. M. Al-Mdallal, A comparative remark on heat transfer in thermally stratified MHD Jeffrey fluid flow with thermal radiations subject to cylindrical/plane surfaces, *Case Stud. Therm. Eng.*, **32**, (2022), 101913. https://doi.org/10.1016/j.csite.2013.08.004
30. A. Alsaedi, K. Muhammad, T. Hayat, Numerical study of MHD hybrid nanofluid flow between two coaxial cylinders, *Alex. Eng. J.*, **61** (2022), 8355–8362. https://doi.org/10.1016/j.aej.2022.01.067
31. S. Bilal, S. U. Mamatha, C. S. K. Raju, B. M. Rao, M. Y. Malik, A. Akgül, Dynamics of chemically reactive Jeffery fluid embedded in permeable media along with influence of magnetic field on associated boundary layers under multiple slip conditions, *Results Phys.*, **28** (2021), 104558. https://doi.org/10.1016/j.rinp.2021.104558
32. M. Arif, P. Kumam, D. Khan, W. Watthayu, Thermal performance of GO-MoS2/engine oil as Maxwell hybrid nanofluid flow with heat transfer in oscillating vertical cylinder, *Case Stud. Therm. Eng.*, **27** (2021), 101290. https://doi.org/10.1016/j.csite.2021.101290
33. M. Turkyilmazoglu, Stagnation-point flow and heat transfer over stretchable plates and cylinders with an oncoming flow: exact solutions, *Chem. Eng. Sci.*, **238** (2021), 116596. https://doi.org/10.1016/j.ces.2021.116596
34. Abbas, S. Nadeem, A. Saleem, M. Y. Malik, A. Issakhov, F. M. Alharbi, Models base study of inclined MHD of hybrid nanofluid flow over nonlinear stretching cylinder, *Chinese J. Phys.*, **69** (2021), 109–117. https://doi.org/10.1016/j.cjph.2020.11.019
35. J. Ahmed, A. Shahzad, A. Farooq, M. Kamran, S. Ud-Din Khan, Thermal analysis in swirling flow of titanium dioxide–aluminum oxide water hybrid nanofluid over a rotating cylinder, *J. Therm. Anal. Calorim.*, **144** (2021), 2175–2185. https://doi.org/10.1007/s10973-020-10190-3

AIMS Press